Recognition of the Protein Kinase AVRPPHB SUSCEPTIBLE1 by the Disease Resistance Protein RESISTANCE TO PSEUDOMONAS SYRINGAE5 Is Dependent on *S*-Acylation and an Exposed Loop in AVRPPHB SUSCEPTIBLE1[1][W][OPEN]

Dong Qi[2], Ullrich Dubiella[2], Sang Hee Kim[2,3], D. Isaiah Sloss, Robert H. Dowen, Jack E. Dixon, and Roger W. Innes*

Department of Biology, Indiana University, Bloomington, Indiana 47405 (D.Q., U.D., S.H.K., D.I.S., R.W.I.); Departments of Pharmacology, Cellular and Molecular Medicine, and Chemistry and Biochemistry and Biomedical Sciences Graduate Program, University of California, San Diego, La Jolla, California 92093 (R.H.D, J.E.D.); and Howard Hughes Medical Institute, Chevy Chase, Maryland 20815 (J.E.D.)

The recognition of pathogen effector proteins by plants is typically mediated by intracellular receptors belonging to the nucleotide-binding leucine-rich repeat (NLR) family. NLR proteins often detect pathogen effector proteins indirectly by detecting modification of their targets. How NLR proteins detect such modifications is poorly understood. To address these questions, we have been investigating the Arabidopsis (*Arabidopsis thaliana*) NLR protein RESISTANCE TO PSEUDOMONAS SYRINGAE5 (RPS5), which detects the *Pseudomonas syringae* effector protein Avirulence protein Pseudomonas phaseolicolaB (AvrPphB). AvrPphB is a cysteine protease that specifically targets a subfamily of receptor-like cytoplasmic kinases, including the Arabidopsis protein kinase AVRPPHB Susceptible1 (PBS1). RPS5 is activated by the cleavage of PBS1 at the apex of its activation loop. Here, we show that RPS5 activation requires that PBS1 be localized to the plasma membrane and that plasma membrane localization of PBS1 is mediated by amino-terminal *S*-acylation. We also describe the development of a high-throughput screen for mutations in *PBS1* that block RPS5 activation, which uncovered four new *pbs1* alleles, two of which blocked cleavage by AvrPphB. Lastly, we show that RPS5 distinguishes among closely related kinases by the amino acid sequence (SEMPH) within an exposed loop in the C-terminal one-third of PBS1. The SEMPH loop is located on the opposite side of PBS1 from the AvrPphB cleavage site, suggesting that RPS5 associates with the SEMPH loop while leaving the AvrPphB cleavage site exposed. These findings provide support for a model of NLR activation in which NLR proteins form a preactivation complex with effector targets and then sense a conformational change in the target induced by effector modification.

Pathogen recognition by plants is mediated by both transmembrane cell surface receptors and intracellular receptors (Jones and Dangl, 2006). The latter receptors typically belong to the nucleotide-binding leucine-rich repeat (NLR) superfamily of proteins, which also play a central role in the innate immune systems of many animals, including humans (von Moltke et al., 2013). In plants, most NLR proteins detect pathogen "effector" proteins, which are proteins secreted by pathogens to promote virulence on susceptible hosts. The immune response activated by NLR proteins is thus referred to as effector-triggered immunity. In the majority of examples studied, effector-triggered immunity is accompanied by localized host cell death around the site of pathogen ingress, which is referred to as the hypersensitive response (HR; Goodman and Novacky, 1994).

Several NLR proteins have been shown to detect pathogen effector proteins indirectly by detecting the modification of other host proteins mediated by the effectors (DeYoung and Innes, 2006). The best characterized examples of NLR proteins that employ indirect recognition mechanisms are the RESISTANCE TO PSEUDOMONAS MACULICOLA1 (RPM1) and RESISTANCE TO PSEUDOMONAS SYRINGAE2 (RPS2) proteins of Arabidopsis (*Arabidopsis thaliana*), which detect modification to the RPM1 INTERACTING4 (RIN4) protein (Mackey et al., 2002; Axtell and Staskawicz, 2003), the RESISTANCE TO PSEUDOMONAS SYRINGAE5 (RPS5) protein of Arabidopsis, which detects modification

[1] This work was supported by the National Institute of General Medical Sciences at the National Institutes of Health (grant no. R01 GM046451 to R.W.I. and grant no. R01 GM090328 to J.E.D.)

[2] These authors contributed equally to the article.

[3] Present address: Division of Plant Sciences, University of Missouri, Columbia, MO 65211.

* Address correspondence to rinnes@indiana.edu.

The author responsible for distribution of materials integral to the findings presented in this article in accordance with the policy described in the Instructions for Authors (www.plantphysiol.org) is: Roger W. Innes (rinnes@indiana.edu).

[W] The online version of this article contains Web-only data.

[OPEN] Articles can be viewed online without a subscription.

www.plantphysiol.org/cgi/doi/10.1104/pp.113.227686

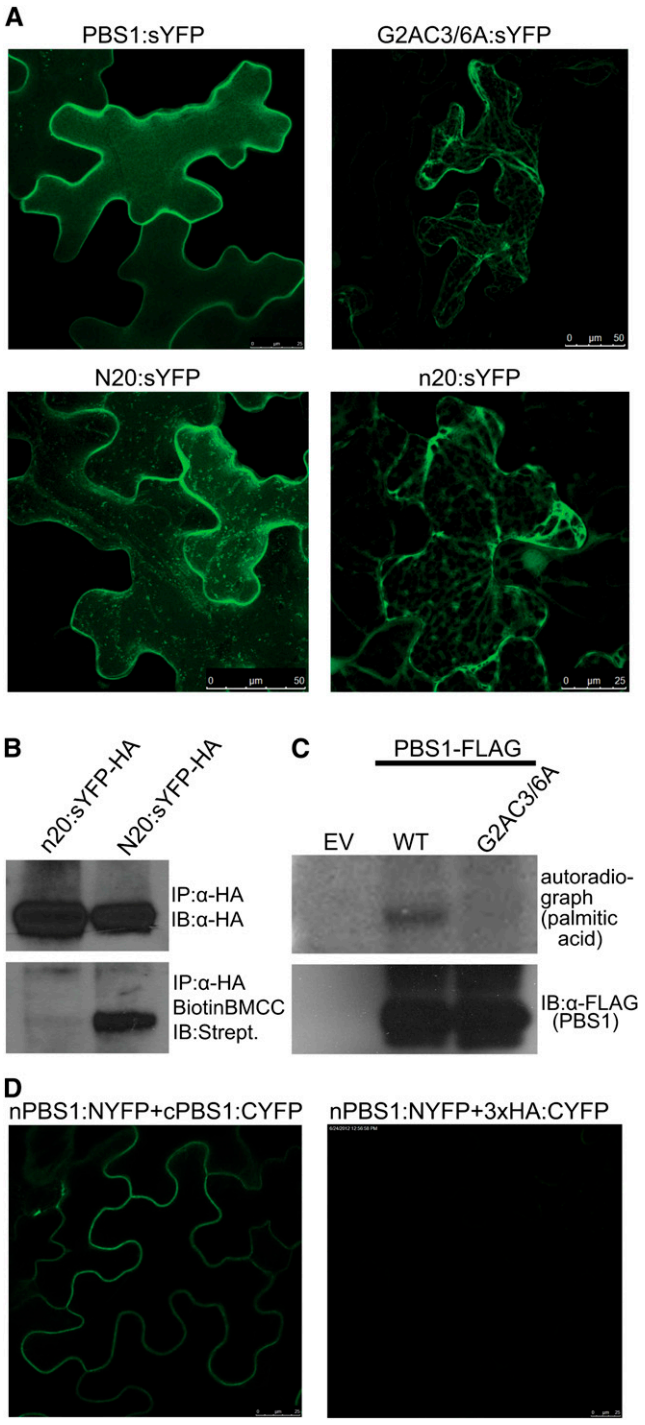

Figure 1. *S*-Acylation mediates PBS1 localization to the PM. A, The predicted N-terminal *S*-acylation motif in PBS1 is necessary and sufficient for localizing PBS1 to the PM. The indicated PBS1 derivatives were fused to sYFP and transiently expressed in *N. benthamiana* leaves using a dexamethasone-inducible promoter. N20 indicates the first 20 amino acids of PBS1, while n20 is the same fragment with the G2AC3/6A triple substitution, which mutates the predicted *S*-acylation site. Confocal laser scanning microscopy was performed at 5 h post dexamethasone induction. All images are three-dimensional projections from a Z-stack. B, PBS1 is *S*-acylated. Cell extracts of *N. benthamiana* tissue expressing N20:sYFP-HA were subjected to immunoprecipitation using α-HA matrix. Immunoprecipitates (IP) were treated with 50 mM *N*-ethylmaleimide to block free sulfhydryl groups, incubated with 1 M hydroxylamine to hydrolyze any Cys-palmitate thioester bonds, and then treated with 1 μM Biotin-BMCC to label free sulfhydryl groups resulting from cleaved thioester bonds. Modified immunoprecipitates were analyzed by immunoblot (IB) with streptavidin-horseradish peroxidase. C, Full-length PBS1 is palmitoylated when expressed in yeast. The indicated PBS1 constructs were expressed in yeast in the presence of [^{3}H]palmitic acid, immunoprecipitated, and separated on an SDS-PAGE gel, and radiolabeling was detected by autoradiography. EV, Empty vector; WT, wild type. D, Engineered PBS1 cleavage products interact with each other at the PM. BiFC was detected between the N-terminal PBS1 cleavage product (nPBS1:NYFP) and the C-terminal PBS1 cleavage product (cPBS1:CYFP) but not between nPBS1:NYFP and 3× HA:CYFP used as a negative control. The indicated constructs were coexpressed in *N. benthamiana* leaves, and imaging was performed at 5 h post dexamethasone induction.

of the AVRPPHB SUSCEPTIBLE1 (PBS1) protein kinase (Ade et al., 2007), and the Pseudomonas resistance and fenthion sensitivity (Prf) protein of tomato (*Solanum lycopersicum*), which detects modification of the *Pseudomonas syringae* pv tomato resistance (Pto) protein kinase (Salmeron et al., 1996; Rathjen et al., 1999). Our group has focused on RPS5, which detects the effector protein Avirulence protein Pseudomonas phaseolicolaB (AvrPphB) from *Pseudomonas syringae* (Simonich and Innes, 1995). AvrPphB functions as a Cys protease (Zhu et al., 2004) and specifically targets a subclass of plant receptor-like cytoplasmic kinases that include PBS1 (Shao et al., 2003; Zhang et al., 2010). AvrPphB likely targets these kinases in order to suppress defense responses induced by cell surface-localized plant immune receptors such as FLAGELLIN SENSITIVE2 (FLS2; Zhang et al., 2010). PBS1 can be coimmunoprecipitated with FLS2, and mutation of *PBS1* reduces FLS2-mediated production of hydrogen peroxide and callose deposits (Zhang et al., 2010), confirming that PBS1 functions in defense signaling.

Cleavage of PBS1 by AvrPphB is both necessary and sufficient to activate RPS5 (Ade et al., 2007), and null mutations in *PBS1* block RPS5 activation (Swiderski and Innes, 2001). Because AvrPphB can cleave multiple closely related kinases in Arabidopsis (Zhang et al., 2010), these observations indicate that RPS5 can distinguish among these kinases, with only PBS1 cleavage activating RPS5. The molecular basis for this specificity is unknown.

One contributor to the specificity of RPS5 may be subcellular localization. RPS5 localizes to the plasma membrane (PM), and amino acid substitutions that displace RPS5 from the PM eliminate RPS5-mediated defense responses (Qi et al., 2012). PBS1 is also expected to localize to the PM, because fusion of the N-terminal 100 amino acids of PBS1 to GFP causes GFP to localize to the PM in both Arabidopsis and *Nicotiana benthamiana* (Takemoto et al., 2012). Consistent with this expectation, PBS1 and RPS5 can be coimmunoprecipitated when transiently overexpressed in *N. benthamiana* (Ade et al., 2007). Furthermore, AvrPphB is both myristoylated and palmitoylated upon entry into plant cells and localizes

to the PM, with PM localization of AvrPphB being required for the activation of RPS5 (Dowen et al., 2009). Although these data all point to a PM localization for PBS1, full-length PBS1 protein has not yet been localized, nor has the functional significance of PBS1 localization been assessed relative to the activation of RPS5.

In this study, we demonstrate that PBS1 is targeted to the PM via *S*-acylation at its N terminus and that PM localization is required for RPS5 activation. We also describe a high-throughput genetic screen for uncovering new mutations in PBS1 that block RPS5 activation, which uncovered four new *pbs1* alleles. Lastly, we show that RPS5 distinguishes PBS1 from closely related kinases based on a specific loop in the C-terminal half of PBS1.

RESULTS

S-Acylation Likely Mediates the PM Localization of Both Full-Length PBS1 and Its Cleavage Products

PBS1 contains a predicted N-terminal *S*-acylation signal (MGCFSCFDS), with both Cys-3 and Cys-6 residues predicted to be palmitoylated by CSS-Palm 3.0 (http://csspalm.biocuckoo.org/; Ren et al., 2008). Consistent with this prediction, a previous study showed that fusion of the first 100 amino acids of PBS1 to GFP causes GFP to localize to the PM (Takemoto et al., 2012). However, this work did not address whether full-length PBS1 localizes to the PM, nor whether Cys-3 and/or Cys-6 are required for PM localization. In this study, we fused super yellow fluorescent protein (sYFP) to the C terminus of full-length PBS1. Laser scanning confocal microscopy imaging demonstrated that PBS1-sYFP localizes to the PM when expressed in *N. benthamiana* epidermal cells (Fig. 1A). Palmitoylation is usually associated with myristoylation at Gly-2 (Batistic et al., 2008), so we created G2A and G2AC3/6A mutations in the PBS1-sYFP fusion to investigate their respective contribution to PBS1 localization. The G2A mutation did not cause a significant change in PBS1 localization (Supplemental Fig. S1A). However, the G2AC3/6A mutation caused significant dissociation of PBS1 from the PM (Fig. 1A). On the other hand, the kinase activity of PBS1 appears not to be necessary for PBS1 PM localization, as the kinase-inactive PBS1, K115N, still showed a typical peripheral PM localization profile (Supplemental Fig. S1B).

To further map the PM localization signal, we fused the first 20 amino acids of PBS1 to sYFP (N20:sYFP). Transient expression of N20:sYFP in *N. benthamiana* revealed a PM localization profile (Fig. 1A). In addition to the PM signal, we observed highly mobile vesicle-like structures. Such structures are frequently observed when acylated proteins are overexpressed (Vilas et al., 2006; Joensuu et al., 2010). A G2AC3/6A mutant form of N20-sYFP (n20:sYFP) accumulated in the cytoplasm instead of PM, indicating that one or more of these residues is required for PM localization (Fig. 1A). To determine whether the Cys-3 and Cys-6 residues of PBS1 are modified through thioester linkage to acyl groups, we assessed protein acylation using a "biotin switch" assay (Hemsley et al., 2008; Hemsley, 2013). This method uses hydroxylamine-induced cleavage of thioester bonds, which results in free sulfhydryl groups that can then be conjugated to a biotin derivative, Biotin-BMCC (see "Materials and Methods"). N20:sYFP transiently expressed in *N. benthamiana* was immunoprecipitated and suspended in *N*-ethylmaleimide to block any free, nonacylated Cys residues, treated with hydroxylamine to cleave thioester bonds, and incubated with Biotin-BMCC to label newly exposed sulfhydryl groups, followed by immunoblot analysis with streptavidin to detect any fatty acid modifications. The N20:sYFP fusion was successfully labeled with biotin, while n20:sYFP with the G2AC3/6A mutation was not (Fig. 1B), indicating that the Cys-3 and/or Cys-6 residues of PBS1 are acylated. To confirm that PBS1 can be acylated with palmitic acid, we performed in vivo labeling of full-length PBS1 in yeast with tritium-labeled palmitic acid. Wild-type PBS1 was labeled, while the G2AC3/6A mutant was not (Fig. 1C).

We have previously shown that RPS5 can be activated by simultaneous expression of the two engineered PBS1 cleavage products, which recapitulates AvrPphB cleavage (DeYoung et al., 2012). Knowledge of the subcellular localization of these two products would thus be helpful for understanding how RPS5 is activated. We generated C-terminal fusions for both the N-terminal PBS1 cleavage product (nPBS1:sYFP) and the C-terminal PBS1 cleavage product (cPBS1:sYFP). Confocal microscopy imaging revealed a PM localization profile for nPBS1:sYFP but a cytosolic and nuclear localization pattern for cPBS1:sYFP (Supplemental Fig. S1C). However, the presence of both PBS1 cleavage products is necessary for RPS5 activation (DeYoung et al., 2012), and PM localization of RPS5 is essential for its activation (Qi et al., 2012), suggesting that there must be a subpopulation of cPBS1 localized to the PM, perhaps via intra-PBS1 contacts. To test this hypothesis, we performed bimolecular fluorescence complementation (BiFC) on the two PBS1 cleavage products. For this purpose, we generated nPBS1:NYFP (for N-terminal half of sYFP) and cPBS1:CYFP (for C-terminal half of sYFP) constructs. Coexpression of these two constructs in *N. benthamiana* produced a strong BiFC signal on the PM (Fig. 1D). As a negative control, we coexpressed nPBS1-NYFP with 3× hemagglutinin (HA)-CYFP, which produced no BiFC signal. The interaction of nPBS1 and cPBS1 in this BiFC assay is consistent with our previous observation that the two engineered cleavage products interact with each other in coimmunoprecipitation assays (DeYoung et al., 2012). Taken together, these data indicate that the two halves of PBS1 remain associated on the PM following cleavage by AvrPphB.

S-Acylation of PBS1 Is Required for RPS5-Mediated Resistance in Arabidopsis

To investigate the importance of PBS1 acylation in RPS5-mediated resistance, we generated transgenic Arabidopsis

plants expressing wild-type PBS1, the G2A mutant, and the G2AC3/6A mutant under the control of the native PBS1 promoter in a *pbs1-1* mutant background. To facilitate subsequent analyses, all constructs were tagged with a C-terminal HA epitope. Similar to plants expressing wild-type PBS1, the G2A-PBS1 transformants showed a strong HR when infiltrated with *P. syringae* strain DC3000(*avrPphB*) at 16 h after inoculation (Fig. 2A). In contrast, both the G2AC3/6A mutant and the empty vector control failed to complement the *pbs1-1* mutation, producing no visible HR (Fig. 2A), indicating that the C3/6A substitutions in PBS1 blocked the activation of RPS5. We confirmed that G2AC3/6A-PBS1 failed to activate RPS5 by measuring bacterial growth. Consistent with the HR data, the growth of DC3000(*avrPphB*) in G2AC3/6A-PBS1 transgenic plants was indistinguishable from that observed in *pbs1-1* control plants transformed with the empty vector and approximately 500-fold higher than in plants transformed with wild-type PBS1 (Fig. 2B). Furthermore, the growth of DC3000(*avrPphB*) in G2AC3/6A-PBS1 plants was similar to that of DC3000 lacking *avrPphB* (Supplemental Fig. S2). Taken together, we conclude that the localization of PBS1 to the PM via Cys-3 and/or Cys-6 acylation is essential for the activation of RPS5 by DC3000(*avrPphB*).

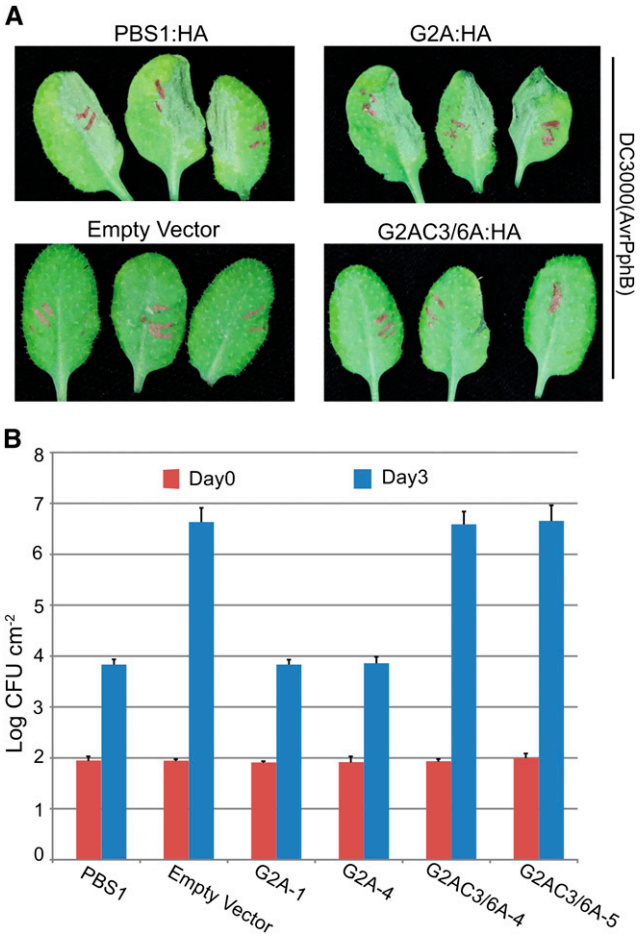

Figure 2. *S*-Acylation of PBS1 is required for RPS5-mediated resistance in Arabidopsis. A, *S*-Acylation of PBS1 is necessary for HR induction by *P. syringae* strain DC3000(*avrPphB*). The *pbs1-1* mutant was transformed with the indicated *PBS1* constructs under the control of the native *PBS1* promoter and then assessed for RPS5-mediated HR by inoculation with DC3000(*avrPphB*). HR was scored at 16 h post inoculation. Plants transformed with empty vector were included as a negative control. B, The PBS1 *S*-acylation mutant is susceptible to *P. syringae* strain DC3000(*avrPphB*). The same transgenic lines were assessed for the growth of DC3000(*avrPphB*) following syringe infiltration. Data shown represent means and SD ($n = 3$). Two independent experiments were performed with similar results, and two independent transgenic lines were tested for each mutant.

Acylation of PBS1 Is Required for Cleavage by Wild-Type AvrPphB

AvrPphB has previously been shown to localize to the PM via N-terminal acylation (Dowen et al., 2009). One possible explanation for the failure of G2AC3/6A-PBS1 to complement the *pbs1-1* mutation is that PBS1 must be associated with the PM to be cleaved by AvrPphB. To test this hypothesis, we injected DC3000 (*avrPphB*) into transgenic plants expressing wild-type PBS1:HA or G2AC3/6A-PBS1:HA and assessed PBS1 cleavage using immunoblot analysis. At 6 h post injection, the C-terminal PBS1 cleavage product was detected in extract from wild-type PBS1:HA tissue (Fig. 3A). In contrast, no PBS1 cleavage was detected in the G2AC3/6A-PBS1:HA tissue injected with DC3000 (*avrPphB*) or in wild-type PBS1:HA tissue injected with DC3000 lacking *avrPphB* (Fig. 3A). In addition, G2AC3/6A-PBS1 accumulated to a level similar to that of wild-type PBS1, indicating that the failure of G2AC3/6A-PBS1 to complement *pbs1-1* (Fig. 2) was not due to poor protein accumulation. To investigate whether the inhibition of PBS1 cleavage by the G2AC3/6A mutation was because of structural constraints or the lack of colocalization, we introduced the G2A mutation into AvrPphB, which has been shown to dissociate AvrPphB from the PM (Dowen et al., 2009). The simultaneous overexpression of G2A-AvrPphB and G2AC3/6A-PBS1 in *N. benthamiana* resulted in PBS1 cleavage, while coexpression with G2A-C98S (a protease-inactive variant of AvrPphB) did not (Fig. 3B), indicating that G2AC3/6A-PBS1 remains a functional substrate for AvrPphB. Taken together, the G2AC3/6A mutation inhibits PBS1 cleavage by AvrPphB by causing PBS1 to localize to a different subcellular compartment from AvrPphB rather than by causing a structural change in PBS1.

Isolation of New Mutant Alleles of *PBS1* That Block AvrPphB-Induced Activation of RPS5

To further investigate the structural requirements for the activation of RPS5 by PBS1 cleavage, we designed an ethyl methanesulfonate (EMS)-induced mutation screen that enabled us to select for mutations in the native *PBS1* gene. For this screen, we generated a transgenic

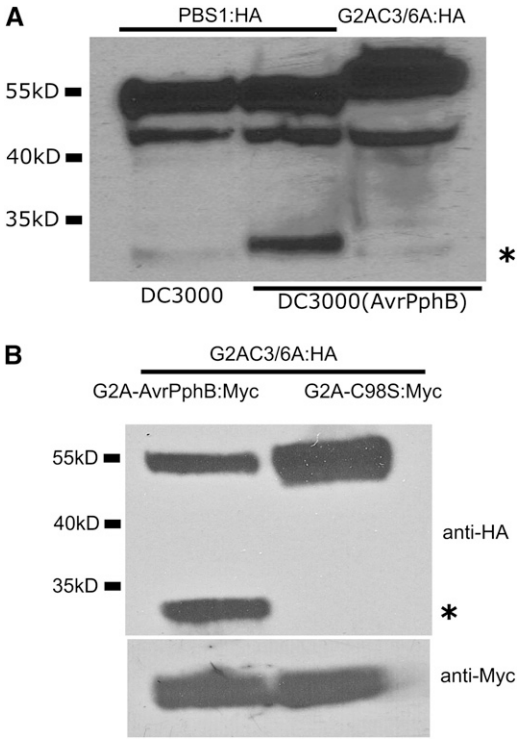

Figure 3. *S*-Acylation of PBS1 is required for cleavage by AvrPphB in vivo. A, *S*-acylation of PBS1 is required for cleavage by AvrPphB delivered by DC3000(*avrPphB*) into plant cells. Transgenic plants expressing wild-type PBS1-HA and the G2AC3/6A mutant were syringe infiltrated with DC3000(*avrPphB*). The infiltrated tissues were harvested 6 h post inoculation and subjected to immunoblot analysis with anti-HA antibodies. Transgenic plants expressing wild-type PBS1 and challenged with DC3000 lacking *avrPphB* were employed as the negative control. B, *S*-Acylation of PBS1 is not structurally required for cleavage by AvrPphB. The G2AC3/6A-PBS1 mutant was transiently coexpressed with a G2A-AvrPphB mutant in *N. benthamiana*, which localizes to the cytoplasm. The C98S mutant of AvrPphB, which lacks protease activity, was included as the negative control. Tissues were harvested at 5 h post dexamethasone induction. Asterisks indicate C-terminal PBS1 cleavage products.

Arabidopsis line that contained *avrPphB* under the control of an estradiol-inducible promoter, which enabled us to activate RPS5 by germinating seedlings on agarose plates containing estradiol, leading to their death (Supplemental Fig. S3A). To avoid obtaining mutations in *RPS5*, we employed a transgenic Arabidopsis line that contained at least two copies of an *RPS5* transgene, reasoning that it would be highly unlikely for EMS to simultaneously inactivate multiple copies. From this screen, we expected to uncover mutations in PBS1 that either blocked the cleavage of PBS1 by AvrPphB or blocked the recognition of cleavage by RPS5. We also expected to uncover mutations in genes required for RPS5-mediated cell death that functioned downstream of RPS5 activation.

We named the above transgenic line EAR5 for estradiol-inducible AvrPphB containing multiple *RPS5* genes. There were no morphological differences between EAR5 and wild-type Columbia (Col-0) plants grown in soil. In addition, in the absence of estradiol induction, the growth of virulent *P. syringae* strain DC3000 or avirulent DC3000(*avrPphB*) in EAR5 plants was indistinguishable from that in wild-type Col-0 plants (Supplemental Fig. S3B). These data indicate that immune responses are not being activated in EAR5 plants prior to induction of the *avrPphB* transgene. As shown in Supplemental Figure S3C, spraying estradiol on EAR5 plants induced massive cell death by 48 h post induction. This response was dependent on RPS5, as a transgenic line containing the same estradiol-inducible *avrPphB* transgene in an *rps5* mutant background remained green and healthy after estradiol induction (data not shown).

We mutagenized EAR5 seeds with EMS and then screened M2 seeds on agar plates for mutants that germinated in the presence of estradiol. We screened approximately 200,000 M2 seeds divided into 98 pools representing approximately 50 M1 parents each. From this screen, we obtained 65 M2 estradiol-resistant mutants (Supplemental Fig. S3D). To confirm that we were not obtaining *rps5* mutants, we sequenced *RPS5* from the first seven mutants isolated from five pools; none had mutations in *RPS5*. Seventeen of the mutants were sterile; thus, 48 mutants from 25 M1 pools were propagated to the M3 generation. Eighteen of the 48 M3 families were found to lack the *avrPphB* transgene and were discarded. The remaining 30 mutants were tested in the M3 generation for the induction of HR following inoculation with *P. syringae* DC3000(*avrPphB*). Nineteen of these lines induced a strong HR, suggesting that these lines contained mutations in the *avrPphB* transgene system that reduced AvrPphB expression or function. Indeed, seven of these lines were found to contain mutations within *avrPphB* (data not shown). The remaining 11 M3 families all displayed a compromised HR in response to *P. syringae* DC3000(*avrPphB*), making these likely candidates for containing mutations in *PBS1*. Sequencing of *PBS1* in these 11 mutants revealed that five contained mutations in *PBS1* (Fig. 4A; Supplemental Fig. S3D), with two of these being identical mutations isolated from the same M2 pool, likely representing siblings.

The four new *pbs1* mutant alleles were named *pbs1-3*, *pbs1-4*, *pbs1-5*, and *pbs1-6*, as the *pbs1-1* and *pbs1-2* alleles have been described previously (Warren et al., 1999; Swiderski and Innes, 2001). All four new alleles contained missense mutations located within the kinase domain of PBS1 (Fig. 4A). To confirm that these mutations blocked the recognition of *P. syringae* expressing *avrPphB*, we inoculated them with *P. syringae* strain DC3000(*avrPphB*) at a density of 5×10^7 colony-forming units (cfu) mL^{-1} and scored for induction of an HR (tissue collapse). As shown in Figure 4B, none of the *pbs1* mutants produced an HR, while the EAR5 parent did. To quantify the level of resistance in the *pbs1* mutants, we performed in planta bacterial growth assays. The growth of DC3000(*avrPphB*) in the four new *pbs1* mutants was similar to that in *pbs1-2* and was approximately 1,000-fold higher than in the EAR5 parent,

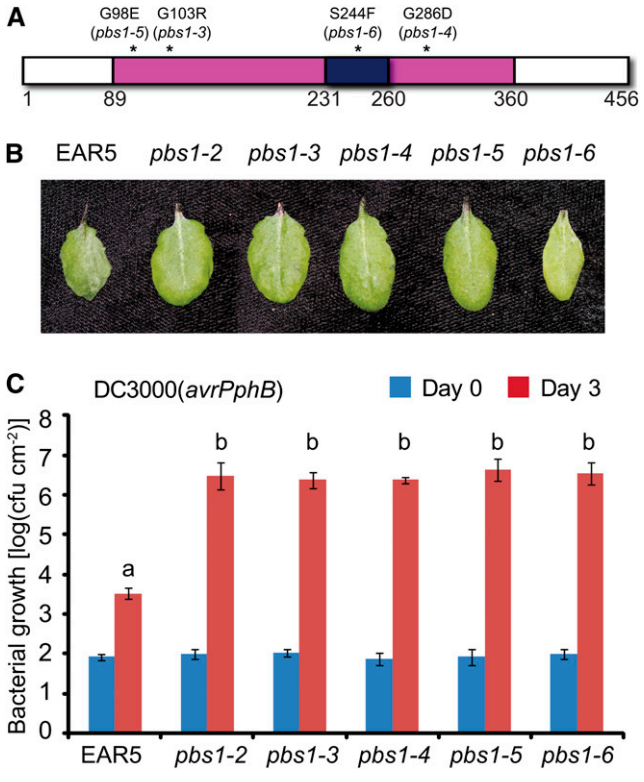

Figure 4. The EAR5 *pbs1* mutants are unable to activate RPS5 in response to *P. syringae* strain DC3000(*avrPphB*). A, Schematic diagram of missense mutations identified in PBS1. The kinase domain and activation segment of PBS1 are represented by pink and dark blue boxes, respectively. Missense substitutions found in mutants are indicated above the bar and marked by asterisks. B, The EAR5 *pbs1* mutants fail to induce HR following inoculation with DC3000(*avrPphB*). Leaves were syringe inoculated with DC3000(*avrPphB*) and photographed 24 h later. C, The EAR5 *pbs1* mutants are susceptible to DC3000(*avrPphB*). Data represent means and SD. Different letters above the bars denote significant differences determined by a two-tailed Student's *t* test ($P < 0.01$). This experiment was repeated twice with similar results.

indicating that all four *pbs1* alleles eliminate AvrPphB recognition (Fig. 4C).

Mutations in *PBS1* could block the activation of RPS5 by several different mechanisms, including destabilizing the PBS1 protein, blocking cleavage by AvrPphB, eliminating kinase activity, and/or blocking the association with RPS5. To assess whether any of the mutations affected stability and/or cleavage by AvrPphB, we transiently coexpressed the *pbs1* mutants with *avrPphB* in *N. benthamiana* and performed immunoblot analyses. The G103R substitution (*pbs1-3*) appeared to destabilize PBS1, as it accumulated poorly (Fig. 5). The G286D (*pbs1-4*), G98E (*pbs1-5*), and S244F (*pbs1-6*) substitutions accumulated to levels slightly less than wild-type PBS1. The G98E and S244F substitutions did not affect cleavage by AvrPphB, while the G103R and G286D substitutions appeared to completely block cleavage (Fig. 5). The G98E substitution is located in the P-loop (Walker A motif) of PBS1 (Fig. 6) and is thus expected to eliminate ATP binding and kinase activity, which likely accounts for its failure to activate RPS5. The S244F substitution is located immediately C terminal of the cleavage site and thus may affect cleavage when AvrPphB is delivered from *P. syringae*. Why G103R and G286D block cleavage is unclear, but this observation suggests that these mutations are disrupting the overall structure of PBS1, which is plausible given that each substitution causes the introduction of a charged side chain in place of no side chain.

RPS5 Distinguishes PBS1 from Closely Related Kinases Based on Polymorphisms in a C-Terminal Loop

To gain further insight into the structural basis of PBS1 recognition by RPS5, we compared the amino acid sequence of RPS5 with those of closely related members of the receptor-like cytoplasmic kinase family that are not recognized by RPS5. The Arabidopsis genome contains 29 PBS1-like (PBL) proteins, with the most similar (PBL27) being 86% identical and 92% similar across the kinase domain (Supplemental Fig. S4). To assess whether PBLs were distinguished based on their ability to be cleaved by AvrPphB, we cloned the five PBL proteins most similar to PBS1 (*PBL5*, *PBL6*, *PBL7*, *PBL23*, and *PBL27*) along with one of the most dissimilar *PBLs* (*PBL9*) and tested for cleavage by AvrPphB using transient coexpression in *N. benthamiana*. Four of the PBL proteins appeared to be cleaved based on the disappearance of the full-length protein (PBL5, PBL7, PBL9, and PBL27), but only PBL27 (the most similar paralog) consistently produced a detectable cleavage product (Supplemental Fig. S4B). The lack of a detectable cleavage product in the other three suggests that the cleavage products are rapidly degraded following cleavage. These same PBLs were also tested for their ability to activate RPS5 in *N. benthamiana* when coexpressed with

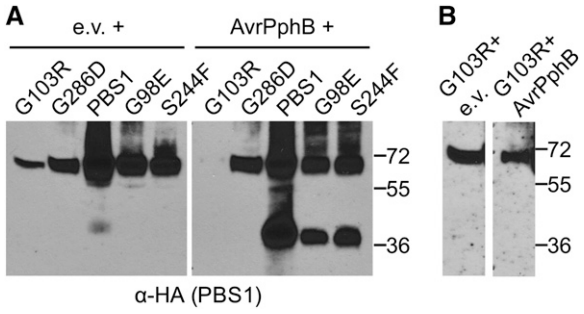

Figure 5. The *pbs1-3* and *pbs1-4* mutations block cleavage by AvrPphB. A, The indicated *pbs1* alleles fused to an HA tag were transiently expressed in *N. benthamiana* in the presence of empty vector (e.v.) or AvrPphB. All constructs were under the control of a dexamethasone-inducible promoter, and samples were prepared 6 h post dexamethasone induction. Cleavage of PBS1 was confirmed by immunoblot analysis with anti-HA antibody. Only G103R (*pbs1-3*) and G286D (*pbs1-4*) were not cleaved by AvrPphB. B, Longer exposure of the immunoblot shown in A to detect G103R. This experiment was repeated twice with similar results.

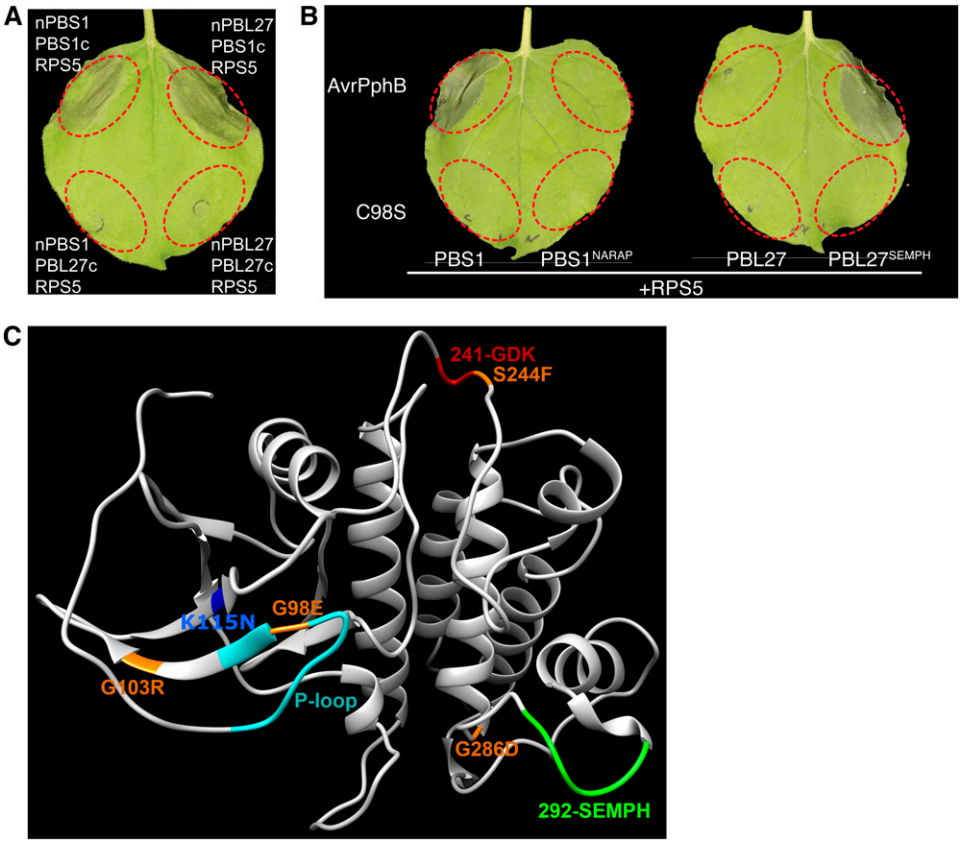

Figure 6. The C-terminal SEMPH motif discriminates between PBS1 and PBL27. A, An HR is induced by coexpression of a PBL27 engineered N-terminal cleavage product together with an engineered C-terminal cleavage product of PBS1 in the presence of RPS5. Red circles mark infiltration sites in *N. benthamiana* leaves. The photograph was taken 16 h after dexamethasone induction. B, Substitution of SEMPH for NARAP in PBL27 enables PBL27 to be recognized by RPS5. The indicated proteins were coexpressed in *N. benthamiana* together with wild-type AvrPphB (+) or its inactive C98S mutant (−) in the presence of RPS5. C, Ribbon diagram of the predicted structure of the PBS1 kinase domain based on alignment with the crystal structure of the tomato Pto kinase (Protein Data Bank accession no. 2QKW). The AvrPphB cleavage site (GDK) is marked in red. The RPS5 recognition motif (SEMPH) is denoted in light green. New PBS1 mutations *pbs1-3* (G103R), *pbs1-4* (G286D), *pbs1-5* (G98E), and *pbs1-6* (S244F) are depicted as amino acid substitutions according to their positions within the molecule (orange). The P-loop is shown in turquoise and Lys-115 is shown in blue. Supplemental Movie S1 shows this diagram rotating in space.

AvrPphB, but none was able to do so (Supplemental Fig. S4C). Together, these results indicate that RPS5 can distinguish among the PBL proteins independent of their ability to be cleaved by AvrPphB.

The high sequence similarity between PBL27 and PBS1 suggested that RPS5 must distinguish between these two proteins based on a small number of amino acid differences. To narrow down the region conferring RPS5 specificity, we took advantage of our finding that RPS5 can be activated in the absence of AvrPphB by coexpression of "engineered" PBS1 cleavage products (i.e. the two halves of PBS1 generated by AvrPphB cleavage; DeYoung et al., 2012). We reasoned that RPS5 specificity might lie in either the N-terminal or C-terminal half of PBS1; therefore, we coexpressed the N-terminal half of PBS1 with the C-terminal half of PBL27 and vice versa and assessed whether RPS5 was activated. HR was observed when the PBL27 N terminus was combined with the PBS1 C terminus in the presence of RPS5 but not when the PBL27 C terminus was used (Fig. 6A). Similar results were observed when using cleavage fragments from a PBS1 homolog from the moss *Physcomitrella patens* (PpPBS1), which also has high sequence similarity to PBS1 (Supplemental Figs. S4 and S5). Only the combination PpPBS1 N terminus plus PBS1 C terminus could trigger RPS5-dependent HR. These findings indicate that the specificity for RPS5 lies within the C-terminal half of PBS1.

Sequence alignment of the kinase domains from PBS1, PBL27, and PpPBS1 revealed a five-amino acid motif in the C-terminal half of the kinase domain that is different in PpPBS1 (NSRAA) and PBL27 (NARAP) compared with PBS1 (SEMPH; Supplemental Fig. S6A). Inspection of the entire Arabidopsis PBL family shown in Supplemental Figure S4 confirmed that SEMPH is unique to PBS1. To test if this motif is necessary for RPS5-triggered HR, we made reciprocal exchanges of the SEMPH and NARAP motifs between PBS1 and PBL27 and coexpressed the

wild-type and mutated proteins together with AvrPphB and RPS5 in *N. benthamiana* (Fig. 6B). The sequence change in PBS1 resulted in a loss of HR, while the introduction of the SEMPH motif into PBL27 enabled RPS5-triggered HR. To exclude the possibility that AvrPphB does not cleave the mutated PBS1 protein, immunoblot analysis was performed (Supplemental Fig. S6B). All proteins were cleaved by AvrPphB. The SEMPH motif is thus a key specificity determinant that enables RPS5 to distinguish PBS1 from closely related kinases.

To gain further insight into the SEMPH motif, we mapped this sequence onto the predicted structure of PBS1 (Fig. 6C; Supplemental Movie S1). Significantly, SEMPH resides on an exposed loop of PBS1. This loop is located on the opposite side of the PBS1 kinase domain from the cleavage site (Lys-243), which suggests that RPS5 may be detecting PBS1 cleavage by sensing the movement of the SEMPH motif following cleavage.

DISCUSSION

The subcellular localization of plant NLR proteins varies between individual NLRs and is likely dictated by the location of the pathogen effector(s) being detected (Qi and Innes, 2013). For NLRs that detect pathogen effectors indirectly, this implies that they should colocalize with specific effector targets. Given that the Arabidopsis NLR protein RPS5 and its corresponding effector, AvrPphB, have previously been shown to localize to the PM (Dowen et al., 2009; Qi et al., 2012), it was expected that PBS1 (an AvrPphB target) would also localize to the PM. Here, we show that this is indeed true. More significantly, we were also able to show that PM localization of PBS1 is dependent on N-terminal *S*-acylation. This acylation is likely to be palmitate (C16), but recent work in Arabidopsis has shown that N-terminal Cys residues can also be modified by the addition of stearate (C18), with both modifications occurring in roughly equal ratios on CALCINEURIN B-LIKE1 (CBL1) and CBL2 (Batistic et al., 2008, 2012).

The process of *S*-acylation in plants is poorly understood, but in the case of CBL1, N-terminal *S*-acylation on Cys-3 was found to be dependent on N-terminal myristoylation on Gly-2, with a G2A substitution blocking acylation on Cys-3 (Batistic et al., 2008). In contrast to CBL1, our data indicate that *S*-acylation of PBS1 is not dependent on Gly-2, with the PBS1 G2A mutant maintaining PM localization (Supplemental Fig. S1A). Indeed, despite the presence of Gly at position 2, the N terminus of PBS1 is not predicted to be myristoylated by either Myristoylator (http://web.expasy.org/myristoylator/; Bologna et al., 2004) or N-Myristoyltransferase-The MYR Predictor (http://mendel.imp.ac.at/myristate/SUPLmain.htm), two common programs used to predict myristoylation sites. We also failed to detect the N-terminal myristoylation of PBS1 experimentally using the same procedures that revealed the myristoylation of AvrPphB (Dowen et al., 2009). Combined with our finding that the first 20 amino acids of PBS1 are sufficient for targeting GFP to the PM (Fig. 1), these data indicate that *S*-acylation of Cys-3 and/or Cys-6 is sufficient for PM localization of PBS1 independent of myristoylation.

S-Acylation likely mediates the PM localization of numerous defense-related proteins in plants. A recent proteomic analysis of *S*-acylated proteins in Arabidopsis revealed over 600 *S*-acylated proteins, including several receptor-like cytoplasmic kinases similar to PBS1, as well as multiple transmembrane receptor-like kinases (Hemsley et al., 2013). Among the latter was the flagellin receptor FLS2. Also included in the list of *S*-acylated proteins were four of the 10 proteins previously found to be associated with the NLR protein RPS2 (Hemsley et al., 2013). The RPS5 protein, which detects the cleavage of PBS1, is also likely to be *S*-acylated, as Cys-4 of RPS5 is predicted to be palmitoylated by CSS-PALM 3.0, and substitution of this residue with Ala disrupts RPS5 PM localization (Qi et al., 2012).

S-Acylation is also required for targeting of AvrPphB to the PM (Dowen et al., 2009). Upon entry into plant cells, AvrPphB self-processes, cleaving itself after Lys-62, generating the new N-terminal sequence GCASSSGVS. Gly-63 is myristoylated and Cys-64 is palmitoylated (Dowen et al., 2009). Substitution of both these residues with Ala dissociates AvrPphB from the PM and prevents the cleavage of PBS1 when AvrPphB is delivered by *P. syringae* and, hence, prevents the activation of RPS5 (Dowen et al., 2009). In conclusion, *S*-acylation plays an essential role in the targeting of PBS1, AvrPphB, and RPS5 to the PM, and this colocalization is required for the recognition of AvrPphB by RPS5. It is noteworthy, however, that AvrPphB can cleave PBS1 in the cytoplasm when acylation-deficient mutants of both are overexpressed together (Fig. 3B); thus, the targeting of AvrPphB to the PM is necessary only to enable AvrPphB to encounter PBS1.

To gain additional insight into how PBS1 cleavage is recognized by RPS5, we conducted a high-throughput mutant screen that was designed to recover mutations in *PBS1* that prevented the activation of RPS5 by AvrPphB. We expected this screen to identify mutations that blocked cleavage by AvrPphB as well as mutations that blocked the recognition of cleavage by RPS5. From this screen, four new *pbs1* missense mutations were identified, all of which eliminated the activation of RPS5 by AvrPphB (Fig. 4). Two of these four (G103R and G286D) blocked cleavage by AvrPphB (Fig. 5). This finding was surprising because both of these residues are located on the opposite side of PBS1 from the cleavage site (Fig. 6). Since both of these substitutions introduce a charged residue, it is plausible that these substitutions induce an overall change in the structure of PBS1. We have previously shown that cleavage of PBS1 by AvrPphB requires that the entire PBS1 kinase domain be intact (i.e. small truncations block cleavage; DeYoung et al., 2012); thus, significant perturbations in the PBS1 structure would be expected to impact cleavage.

Two of the four new *pbs1* alleles (G98E and S244F) did not affect cleavage by AvrPphB in *N. benthamiana*

transient assays but blocked the activation of RPS5 in Arabidopsis. Interestingly, coexpression of the S244F or G98E mutant with AvrPphB and RPS5 in *N. benthamiana* induced a delayed HR (data not shown), indicating that these substitutions do not block RPS5 activation if AvrPphB and PBS1 are overexpressed. Since Ser-244 is located at the AvrPphB cleavage site, we speculate that this substitution may affect cleavage efficiency and, under native levels of AvrPphB, reduce the amount of cleavage below that needed to activate RPS5. The G98E substitution is predicted to inhibit ATP binding, as Gly-98 is located within the P-loop (Walker A motif) of PBS1 (Fig. 6), which is involved in binding the γ-phosphate of ATP. We have previously shown that mutation of Lys-115 of PBS1 (K115N), which forms part of the ATP-binding pocket, blocks PBS1 kinase activity and blocks RPS5 activation in Arabidopsis under native protein levels (Shao et al., 2003), but this mutation does not block RPS5 activation when overexpressed in *N. benthamiana* (Ade et al., 2007). These results suggest that ATP binding by PBS1 promotes the association with and/or recognition by RPS5, which is essential under native protein levels but can be bypassed by overexpression.

As an alternative approach to identifying key residues of PBS1 required for recognition by RPS5, we compared the PBS1 sequence with closely related kinases in Arabidopsis that share with PBS1 predicted N-terminal palmitoylation motifs and, thus, are also likely localized to the PM. These comparisons revealed a polymorphic loop (SEMPH) located between Ser-292 and His-296 of PBS1 (Fig. 6). Swapping this loop into the equivalent position of the kinase most similar to PBS1, PBL27, enabled PBL27 to activate RPS5 upon cleavage by AvrPphB, demonstrating that RPS5 distinguishes between PBS1 and PBL27 based on the amino acids in this loop. This loop is located on the opposite side of PBS1 from the AvrPphB cleavage site, which suggests that RPS5 associates with this side of PBS1, leaving the cleavage site exposed. We speculate that cleavage of PBS1 causes a conformational change in PBS1 that changes the orientation of this loop. This hypothesis is supported by our recent finding that insertion of three, five, or seven amino acids at the AvrPphB cleavage site of PBS1 activates RPS5 in the absence of cleavage (DeYoung et al., 2012). Based on the structural model shown in Figure 6, such an insertion might be expected to act as a wedge that would push the two lobes of PBS1 together on the side of PBS1 opposite to the cleavage site. Confirmation of this model, however, will require crystal structures of the modified and wild-type PBS1 proteins.

With the finding that the SEMPH loop of PBS1 is critical to its recognition by RPS5, we assessed whether this loop is conserved in putative orthologs of PBS1 in other plant species. Although PBS1 is one of the most highly conserved defense genes in plants (Caldwell and Michelmore, 2009), Arabidopsis diverges from most other species in the SEMPH loop, with most species having STRPH in this position (Supplemental Fig. S7). Only the closely related mustard species *Capsella rubella* shared this sequence among kinase sequences in the National Center for Biotechnology Information nonredundant protein database. This observation suggests that Arabidopsis RPS5 will not function in plant species outside the mustard family unless it is coexpressed with Arabidopsis *PBS1*. This likely explains why the *N. benthamiana* ortholog of *PBS1* (PGSC0003DMP400014933) does not substitute for Arabidopsis *PBS1* when we conduct our transient expression assays, as it contains STKPQ at this position.

CONCLUSION

In plants, NLR proteins often detect pathogen effectors indirectly by detecting the effector-induced modification of other host proteins (Innes, 2004). The molecular mechanisms by which NLR proteins sense such modifications are mostly unknown. The work reported above provides two important insights into this process. First, PM localization of defense proteins, including receptor-like cytoplasmic kinases and NLR proteins, is often mediated by *S*-acylation. Indeed, the PM-localized NLR protein RPS2 is predicted to be *S*-acylated on Cys-11 by CSS-PALM, which we predict, based on the work presented here, to be important for the proper localization and function of RPS2. Such *S*-acylation helps ensure colocalization of the NLR and effector target. Second, the RPS5 NLR distinguishes among closely related protein kinases based on a specific exposed loop that varies among kinases. This specificity suggests that this portion of PBS1 may directly interact with RPS5, at least following AvrPphB cleavage, and that RPS5 is detecting the movement of the SEMPH loop rather than detecting the cleavage site. This inference further supports our model that NLR proteins can sense the modification of effector targets by sensing subtle conformational changes rather than directly detecting specific modifications such as phosphorylation or proteolytic cleavage (DeYoung et al., 2012).

MATERIALS AND METHODS

Plant Materials, Growth Conditions, and Pathogenesis Assays

Arabidopsis (*Arabidopsis thaliana*) and *Nicotiana benthamiana* plants were grown in Metro-Mix 360 potting mixture (Sun Gro Horticulture) under a 9-h-light/15-h-dark cycle at 150 μmol m^{-2} s^{-1} and 23°C. The *pbs1-1* and *pbs1-2* mutants have been described previously (Swiderski and Innes, 2001). For HR assays in Arabidopsis, *Pseudomonas syringae* strain DC3000(*avrPphB*) was grown on King's medium B agar, resuspended in 10 mM $MgCl_2$, and infiltrated into leaves of 5-week-old plants using a needless syringe at 5×10^7 cfu mL^{-1} (optical density at 600 nm [OD_{600}] = 0.05). The HR was scored and photographs were taken 24 h after inoculation. To measure bacterial growth in Arabidopsis, leaves of 5-week-old Arabidopsis plants were infiltrated with DC3000 (*avrPphB*) at 10^5 cfu mL^{-1}. Leaf discs totaling 0.5 cm^2 were removed with a cork borer, ground in 10 mM $MgCl_2$, and plated by serial dilution on selective medium in three replicates at the indicated time points.

Construction of Plant Expression Vectors

All constructs used in this study were generated using a modified multisite Gateway cloning system (Invitrogen) as described previously (Qi et al., 2012).

PBS1 and AvrPphB derivatives were PCR amplified from a wild-type PBS1 plasmid template with primers containing the desired mutations (Supplemental Table S1) and cloned into the donor vector pBSDONR P1-P4 (Qi et al., 2012) using Gateway BP Clonase (Life Technologies). Engineered PBS1 cleavage products were cloned by amplifying the corresponding regions of the PBS1 open reading frame (nucleotides 1–729 for the N-terminal product and 730–1,368 for the C-terminal product). Fusion of sYFP with the N-terminal 20 amino acids of PBS1 was created by PCR amplification with an ultramer forward primer comprising the corresponding coding sequence of PBS1 and the first 18 nucleotides of sYFP. All constructs were cloned into pBSDONR P1-P4. 5× Myc, 3× HA, and sYFP tags in the donor vector pBSDONR P4r-P2 have been described previously (Qi et al., 2012). To create protein fusions with epitope tags or fluorescent proteins, the desired "P1-P4" clone, "P4r-P2" clone, and destination vector containing attR1 and attR2 sites were mixed approximately in a 2:2:1 M ratio, and recombination was accomplished by the addition of Gateway LR Clonase II (Life Technologies) and incubation at room temperature overnight.

To create the estradiol-inducible *avrPphB* construct, the estradiol-inducible Gateway destination cassette of pMDC7 (Curtis and Grossniklaus, 2003) was subcloned into the multicloning site of pGREENII0229 (Hellens et al., 2000) to generate the pGRIIesdl estradiol-inducible expression vector with a Basta-selectable marker for plant transformation. The *avrPphB* gene in pBSDONR P1-P4 and the 5× Myc tag in pBSDONR P4r-P2 were recombined with pGRIIesdl using Gateway LR Clonase II. All constructs were sequenced for verification.

Site-directed mutagenesis PCR was performed using a pBSDONR PBS1 template to generate G103R, G286D, G98E, S244F, and SEMPH-to-NARAP exchange entry clones. pBSDONR PBL27 was used as a template for site-directed mutagenesis to generate a NARAP-to-SEMPH exchange. The entry clones and 3× HA were recombined into a pTA7002 destination vector (carrying a dexamethasone-inducible promoter) using Gateway LR Clonase II (Aoyama and Chua, 1997). All constructs were verified by sequencing. Primer sequences used in cloning are listed in Supplemental Table S1.

Transient Expression Assays in *N. benthamiana*

Transient expression assays were performed as described previously (DeYoung et al., 2012). Briefly, dexamethasone-inducible constructs were mobilized into *Agrobacterium tumefaciens* strain GV3101(pMP90). After overnight culture in Luria-Bertani medium, cells were pelleted and resuspended in 10 mM $MgCl_2$ with 100 μM acetosyringone (Sigma-Aldrich). For single construct expression, the suspensions were diluted to OD_{600} = 0.3 before infiltration. For coexpression of multiple constructs, suspensions were mixed in equal ratios before infiltration such that each strain was present at an OD_{600} of 0.3 in the final mixture. The cells was incubated for 2 h at room temperature and infiltrated into leaves of 4-week-old *N. benthamiana* plants. Transgenes were induced by spraying leaves with 50 μM dexamethasone 40 h after inoculation. Samples were harvested for protein extraction 4 to 6 h after dexamethasone application. Laser scanning confocal microscopy was performed at 6 to 8 h after dexamethasone application, unless stated otherwise.

Immunoprecipitation and Immunoblotting

For total protein extraction, six infiltrated leaves were ground in lysis buffer (50 mM Tris, pH 7.5, 150 mM NaCl, 0.1% [v/v] Nonidet P-40, and 1% [v/v] Plant Proteinase Inhibitor Cocktail [Sigma-Aldrich]). Homogenates were centrifuged twice at 13,000 rpm at 4°C for 10 min, and supernatants were transferred to new tubes. For immunoblots, crude extracts were mixed with 4× SDS loading buffer (50 mM Tris-HCl, pH 6.8, 2% (w/v) SDS, 10% (v/v) glycerol, 1% (v/v) β-mercaptoethanol, 12.5 mM EDTA, and 0.02% (w/v) bromphenol blue) at a ratio of 3:1 and boiled for 10 min before resolving by SDS-PAGE. Immunoprecipitations were performed as described previously (Ade et al., 2007) using an anti-HA monoclonal antibody matrix (Roche). All protein samples were resolved on 4% to 20% (w/v) gradient Tris-HEPES-SDS polyacrylamide gels (Thermo Scientific) and transferred to a nitrocellulose membrane for probing with anti-c-Myc peroxidase (Roche), anti-HA peroxidase (Sigma), or streptavidin peroxidase (Pierce). The ImmunoStar HRP Substrate Kit (Bio-Rad) was used for detecting antibody complexes.

Detection of *S*-Acylation

The in vitro detection of PBS1 *S*-acylation was performed as described by Berzat et al. (2005). Briefly, immunoprecipitate of N20-sYFP:HA or n20-sYFP:HA was treated with 50 mM *N*-ethylmaleimide (Sigma-Aldrich) in lysis buffer for 48 h to block free sulfhydryl groups. Immunoprecipitates were then washed, treated for 1 h with 1 M hydroxylamine (Sigma-Aldrich) to hydrolyze any Cys-palmitate or Cys-stearate thioester bonds, washed, and then treated with 1 μM EZ-Link Biotin-BMCC {1-biotinamido-4-[4′-(maleimidomethyl)cyclohexanecarboxamido] butane; Pierce} in 50 mm Tris, pH 7.0, for 2 h to label cleaved thioester bonds. Immunoprecipitates were washed, resuspended in nonreducing protein sample buffer (10% [w/v] SDS, 1 M Tris-HCl, pH 6.8, 25% [w/v] Suc, and 0.01% [w/v] bromphenol blue), resolved by SDS-PAGE, and transferred to a nitrocellulose membrane. Membranes were probed with streptavidin-horseradish peroxidase (Pierce) to detect the incorporation of biotin.

Labeling of PBS1 with [^{3}H]Palmitic Acid in Yeast

In vivo labeling of *Saccharomyces cerevisiae* with [^{3}H]palmitic acid was performed as described previously (Dowen et al., 2009). Briefly, C-terminal 2× FLAG-tagged PBS1 was expressed under the control of a Gal-inducible promoter. Yeast strains were grown to midlog phase in Yeast Extract Peptone Adenine Dextrose media and then diluted (5:50 mL) into complete minimal medium containing 3% raffinose and grown to stationary phase. Approximately 1.7×10^9 cells were then resuspended in 100 mL of rich medium (1% [w/v] bacto yeast extract, 2% [w/v] bacto peptone, and 4% [w/v] Gal) and grown for 4 h at 30°C. Cells (approximately 1×10^9) were resuspended in 25 mL of rich medium containing 3% (w/v) Gal, 3 μg mL^{-1} cerulenin (Sigma-Aldrich), and 50 μCi mL^{-1} [^{3}H]palmitic acid (Perkin-Elmer Life Sciences). Yeast was labeled for 4 h at 30°C before harvesting. Cells were then lysed, PBS1 immunoprecipitated, and subjected to SDS-PAGE. The gel was then treated with Amplify (Amersham Biosciences) to enhance the tritium signal before drying. The gel was analyzed by autoradiography (10-month exposure). To determine protein expression, identical samples were analyzed by immunoblotting with an anti-FLAG M2 peroxidase conjugate antibody (Sigma).

Generation of PBS1 Transgenic Plants

An Arabidopsis PBS1 genomic clone was isolated from Col-0 genomic DNA as described previously (Shao et al., 2003), tagged with a 3× HA epitope directly upstream of the stop codon, and G2A and G2A/C3A/C6A amino acid substitutions were introduced by site-directed mutagenesis. The resulting clones were then placed in the binary vector pJHA212B and transformed into *pbs1-1* plants via *A. tumefaciens*-mediated floral dipping (Clough and Bent, 1998). T1 *pbs1-1*:PBS1-HA plants were isolated by Basta selection in soil.

Confocal Laser Scanning Microscopy

Confocal laser scanning microscopy was performed on an SP5 AOBS inverted confocal microscope (Leica Microsystems) equipped with a 63×, numerical aperture-1.2 water objective. sYFP fusions were excited with a 514-nm argon laser and detected using a 522- to 545-nm band-pass emission filter. To obtain three-dimensional images, a series of Z-stack images were collected and then combined and processed using the three-dimensional image-analysis software IMARIS 7.0 (Bitplane Scientific Software; http://www.bitplane.com).

Mutagenesis and Mutant Screen

The *RPS5*:*HPB* transgenic line (*pRPS5*:*RPS5*:*HPB*/*rps5*) was a kind gift from Fumiaki Katagiri (University of Minnesota; Qi and Katagiri, 2009). The EAR5 transgenic plant was generated by transforming the estradiol-inducible *avrPphB* construct described above into the *RPS5*:*HPB* background. EAR5 seeds were treated with 0.2% EMS (Sigma-Aldrich) for 16 h with gentle agitation. Mutagenized M1 plants were grown under long days in a greenhouse and allowed to self-fertilize. M2 seeds were collected from pools of approximately 50 M1 parents, generating a total of 98 M2 pools. Approximately 200,000 M2 seeds from 98 pools were screened on one-half-strength Murashige and Skoog agar plates containing 20 μM estradiol. Surviving plants were transferred to soil 10 d after germination.

PBS1 Phylogenetic Analyses and Structural Modeling

Phylogenetic analyses were conducted using MEGA5 (Tamura et al., 2011). Full-length protein sequences were aligned using ClustalW, and a sequence similarity tree was created using the neighbor-joining algorithm (Saitou and Nei, 1987). Boostrap values were calculated from 1,000 replicates. The

structure of PBS1 was modeled as described previously using the crystal structure of the tomato (*Solanum lycopersicum*) Pto kinase (Protein Data Bank accession no. 2QKW) as a template (DeYoung et al., 2012).

Sequence data from this article can be found in the GenBank/EMBL data libraries under accession numbers NC_003070 (RPS5), NC_003076 (PBS1), NP_001184932 (PBL5), NP_180426 (PBL6), NP_195900 (PBL7), NP_001184929 (PBL9), NP_188689 (PBL23), NP_001190331 (PBL27), and AJ870974 (AvrPphB).

Supplemental Data

The following materials are available in the online version of this article.

Supplemental Figure S1. Localization of PBS1 derivatives.

Supplemental Figure S2. Mutation of the PBS1 *S*-acylation site does not affect the susceptibility of Arabidopsis to *P. syringae* strain DC3000 lacking AvrPphB.

Supplemental Figure S3. Isolation of new *pbs1* alleles using an estradiol-inducible AvrPphB expression system.

Supplemental Figure S4. PBS1 paralogs cannot substitute for PBS1 in the activation of RPS5 in *N. benthamiana* transient assays.

Supplemental Figure S5. The moss PBS1 N-terminal cleavage product (nPpPBS1) can substitute for the PBS1 N-terminal cleavage product.

Supplemental Figure S6. Mutation of the C-terminal SEMPH motif in PBS1 does not affect cleavage by AvrPphB.

Supplemental Figure S7. Alignment of the PBS1 SEMPH loop region from *PBS1* orthologs from the National Center for Biotechnology Information nonredundant protein database.

Supplemental Table S1. Primer sequences used in this study.

Supplemental Movie S1. Model of PBS1 rotating in space.

ACKNOWLEDGMENTS

We thank Yiping Qi and Fumi Katagiri for providing the RPS5-HPB transgenic Arabidopsis line, and the Indiana University Light Microscopy Imaging Center, which was established by the Indiana METACyt Initiative and the Indiana University Office of the Vice Provost for Research.

Received August 29, 2013; accepted November 12, 2013; published November 13, 2013.

LITERATURE CITED

Ade J, DeYoung BJ, Golstein C, Innes RW (2007) Indirect activation of a plant nucleotide binding site-leucine-rich repeat protein by a bacterial protease. Proc Natl Acad Sci USA **104:** 2531–2536

Aoyama T, Chua NH (1997) A glucocorticoid-mediated transcriptional induction system in transgenic plants. Plant J **11:** 605–612

Axtell MJ, Staskawicz BJ (2003) Initiation of RPS2-specified disease resistance in Arabidopsis is coupled to the AvrRpt2-directed elimination of RIN4. Cell **112:** 369–377

Batistic O, Rehers M, Akerman A, Schlücking K, Steinhorst L, Yalovsky S, Kudla J (2012) S-Acylation-dependent association of the calcium sensor CBL2 with the vacuolar membrane is essential for proper abscisic acid responses. Cell Res **22:** 1155–1168

Batistic O, Sorek N, Schültke S, Yalovsky S, Kudla J (2008) Dual fatty acyl modification determines the localization and plasma membrane targeting of CBL/CIPK Ca^{2+} signaling complexes in *Arabidopsis*. Plant Cell **20:** 1346–1362

Berzat AC, Buss JE, Chenette EJ, Weinbaum CA, Shutes A, Der CJ, Minden A, Cox AD (2005) Transforming activity of the Rho family GTPase, Wrch-1, a Wnt-regulated Cdc42 homolog, is dependent on a novel carboxyl-terminal palmitoylation motif. J Biol Chem **280:** 33055–33065

Bologna G, Yvon C, Duvaud S, Veuthey AL (2004) N-terminal myristoylation predictions by ensembles of neural networks. Proteomics **4:** 1626–1632

Caldwell KS, Michelmore RW (2009) *Arabidopsis thaliana* genes encoding defense signaling and recognition proteins exhibit contrasting evolutionary dynamics. Genetics **181:** 671–684

Clough SJ, Bent AF (1998) Floral dip: a simplified method for Agrobacterium-mediated transformation of *Arabidopsis thaliana*. Plant J **16:** 735–743

Curtis MD, Grossniklaus U (2003) A Gateway cloning vector set for high-throughput functional analysis of genes in planta. Plant Physiol **133:** 462–469

DeYoung BJ, Innes RW (2006) Plant NBS-LRR proteins in pathogen sensing and host defense. Nat Immunol **7:** 1243–1249

DeYoung BJ, Qi D, Kim SH, Burke TP, Innes RW (2012) Activation of a plant nucleotide binding-leucine rich repeat disease resistance protein by a modified self protein. Cell Microbiol **14:** 1071–1084

Dowen RH, Engel JL, Shao F, Ecker JR, Dixon JE (2009) A family of bacterial cysteine protease type III effectors utilizes acylation-dependent and -independent strategies to localize to plasma membranes. J Biol Chem **284:** 15867–15879

Goodman RN, Novacky AJ, editors (1994) The Hypersensitive Reaction in Plants to Pathogen. APS Press, St. Paul

Hellens RP, Edwards EA, Leyland NR, Bean S, Mullineaux PM (2000) pGreen: a versatile and flexible binary Ti vector for Agrobacterium-mediated plant transformation. Plant Mol Biol **42:** 819–832

Hemsley PA (2013) Assaying protein S-acylation in plants. Methods Mol Biol **1043:** 141–146

Hemsley PA, Taylor L, Grierson CS (2008) Assaying protein palmitoylation in plants. Plant Methods **4:** 2

Hemsley PA, Weimar T, Lilley KS, Dupree P, Grierson CS (2013) A proteomic approach identifies many novel palmitoylated proteins in Arabidopsis. New Phytol **197:** 805–814

Innes RW (2004) Guarding the goods: new insights into the central alarm system of plants. Plant Physiol **135:** 695–701

Joensuu JJ, Conley AJ, Lienemann M, Brandle JE, Linder MB, Menassa R (2010) Hydrophobin fusions for high-level transient protein expression and purification in *Nicotiana benthamiana*. Plant Physiol **152:** 622–633

Jones JD, Dangl JL (2006) The plant immune system. Nature **444:** 323–329

Mackey D, Holt BF III, Wiig A, Dangl JL (2002) RIN4 interacts with *Pseudomonas syringae* type III effector molecules and is required for RPM1-mediated resistance in Arabidopsis. Cell **108:** 743–754

Qi D, DeYoung BJ, Innes RW (2012) Structure-function analysis of the coiled-coil and leucine-rich repeat domains of the RPS5 disease resistance protein. Plant Physiol **158:** 1819–1832

Qi D, Innes RW (2013) Recent advances in plant NLR structure, function, localization, and signaling. Front Immunol **4:** 348

Qi Y, Katagiri F (2009) Purification of low-abundance Arabidopsis plasma-membrane protein complexes and identification of candidate components. Plant J **57:** 932–944

Rathjen JP, Chang JH, Staskawicz BJ, Michelmore RW (1999) Constitutively active Pto induces a Prf-dependent hypersensitive response in the absence of avrPto. EMBO J **18:** 3232–3240

Ren J, Wen L, Gao X, Jin C, Xue Y, Yao X (2008) CSS-Palm 2.0: an updated software for palmitoylation sites prediction. Protein Eng Des Sel **21:** 639–644

Saitou N, Nei M (1987) The neighbor-joining method: a new method for reconstructing phylogenetic trees. Mol Biol Evol **4:** 406–425

Salmeron JM, Oldroyd GE, Rommens CM, Scofield SR, Kim HS, Lavelle DT, Dahlbeck D, Staskawicz BJ (1996) Tomato Prf is a member of the leucine-rich repeat class of plant disease resistance genes and lies embedded within the Pto kinase gene cluster. Cell **86:** 123–133

Shao F, Golstein C, Ade J, Stoutemyer M, Dixon JE, Innes RW (2003) Cleavage of Arabidopsis PBS1 by a bacterial type III effector. Science **301:** 1230–1233

Simonich MT, Innes RW (1995) A disease resistance gene in Arabidopsis with specificity for the *avrPph3* gene of *Pseudomonas syringae* pv. *phaseolicola*. Mol Plant Microbe Interact **8:** 637–640

Swiderski MR, Innes RW (2001) The Arabidopsis *PBS1* resistance gene encodes a member of a novel protein kinase subfamily. Plant J **26:** 101–112

Takemoto D, Rafiqi M, Hurley U, Lawrence GJ, Bernoux M, Hardham AR, Ellis JG, Dodds PN, Jones DA (2012) N-terminal motifs in some plant disease resistance proteins function in membrane attachment and contribute to disease resistance. Mol Plant Microbe Interact **25:** 379–392

Tamura K, Peterson D, Peterson N, Stecher G, Nei M, Kumar S (2011) MEGA5: molecular evolutionary genetics analysis using maximum likelihood, evolutionary distance, and maximum parsimony methods. Mol Biol Evol **28:** 2731–2739

Vilas GL, Corvi MM, Plummer GJ, Seime AM, Lambkin GR, Berthiaume LG (2006) Posttranslational myristoylation of caspase-activated p21-activated

protein kinase 2 (PAK2) potentiates late apoptotic events. Proc Natl Acad Sci USA **103:** 6542–6547

von Moltke J, Ayres JS, Kofoed EM, Chavarría-Smith J, Vance RE (2013) Recognition of bacteria by inflammasomes. Annu Rev Immunol **31:** 73–106

Warren RF, Merritt PM, Holub E, Innes RW (1999) Identification of three putative signal transduction genes involved in *R* gene-specified disease resistance in Arabidopsis. Genetics **152:** 401–412

Zhang J, Li W, Xiang T, Liu Z, Laluk K, Ding X, Zou Y, Gao M, Zhang X, Chen S, et al (2010) Receptor-like cytoplasmic kinases integrate signaling from multiple plant immune receptors and are targeted by a *Pseudomonas syringae* effector. Cell Host Microbe **7:** 290–301

Zhu M, Shao F, Innes RW, Dixon JE, Xu Z (2004) The crystal structure of *Pseudomonas* avirulence protein AvrPphB: a papain-like fold with a distinct substrate-binding site. Proc Natl Acad Sci USA **101:** 302–307